Science of the Total Environment 858 (2023) 160045

Contents lists available at ScienceDirect

Science of the Total Environment

journal homepage: www.elsevier.com/locate/scitotenv

Causes & effects of upstream-downstream flow regime alteration over Catchment-Estuary-Coastal systems

Aziza Baubekova [a,*], Mahdi Akbari [a], Hana Etemadi [b], Faisal Bin Ashraf [c], Aliakbar Hekmatzadeh [d], Ali Torabi Haghighi [a]

[a] Water, Energy and Environmental Engineering Research Unit, University of Oulu, Finland
[b] Environmental Science, Persian Gulf Research Institute, Persian Gulf University, Bushehr, Iran
[c] Stockholm Environment Institute, Stockholm, Sweden
[d] Shiraz University of Technology, Iran

HIGHLIGHTS

- Coupling the catchment and coastal processes uncovers the complexity of estuary ecotone.
- The catchment-level study covers climate, land use, and damming impact on the estuary.
- Hydrological alteration at the outlet is lower than at unregulated upstream gauges.
- Low water consumption in the mid-basin allows recovery of the downstream flow regime.
- The impact of climate change on the coastal area is higher than upstream regulation.

GRAPHICAL ABSTRACT

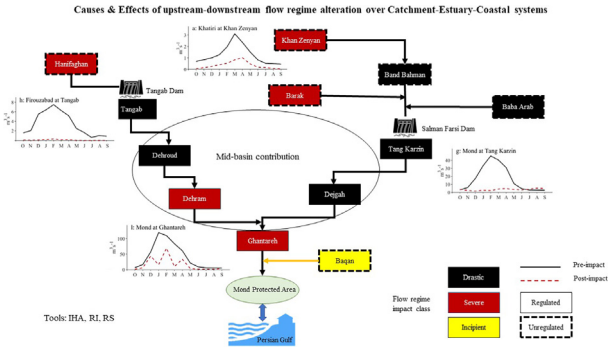

ARTICLE INFO

Editor: Fernando A.L. Pacheco

Keywords:
Flow regime alteration
Catchment-Estuary-Coastal systems
Climate change
River regulation
Mond River
NDVI

ABSTRACT

The construction of large dams along rivers has significantly changed the natural flow regime, reducing the inflow into many lakes and terminal wetlands. However, the question of the impact of dam operation on downstream estuarine wetlands has less been taken into account. Spatio-temporal flow regime alteration in the Mond River shows the complexity of drivers affecting the estuary-coastal system named the Mond-Protected Area in southern Iran. To this end, we applied river impact (RI) and Indicator of hydrological alteration (IHA) methods on monthly and daily river flow data across the basin. Based on the river impact method, a "drastic" impact below two in-operation (Tangab and Salman Farsi) dams, with RI values of 0.02 and 0.08, diminish to a 'severe' impact with RI value of 0.35 at the last gauge (Ghantareh) on the main corridor of the Mond river due to the addition of flow from a large mid-basin (about 20,254 km^2). Furthermore, the degree of hydrological alteration (daily flow analysis) at mid-stream (e.g., Dehram gauges) was similar to the unregulated upstream tributaries (e.g., Hanifaghan gauges). The remote sensing analysis in the Mond Protected Area showed the prevailing impact of sea-level rise in the Persian Gulf with the inundation of the coastal area and a shift of vegetation in a landward direction which complied with standardized precipitation index (SPI) values as a meteorological drought indicator. Thus, the consequence of climate change (e.g., sea-level rise, draught) has a higher impact on the protected area than the upstream river regulation and land-use change in the Mond basin. The holistic approach and the catchment-level study allowed us to see the complexity of the drivers influencing the estuary-coastal system.

* Corresponding author at: Water, Energy and Environmental Engineering, Faculty of Technology, University of Oulu, 90014 Oulu, Finland.
E-mail address: aziza.baubekova@oulu.fi (A. Baubekova).

http://dx.doi.org/10.1016/j.scitotenv.2022.160045
Received 3 September 2022; Received in revised form 26 October 2022; Accepted 4 November 2022
Available online 11 November 2022

1. Introduction

Hard engineering water management projects like dams tend to impact river flow and morphology significantly and have serious implications on the surrounding aquatic and terrestrial habitats (Poff and Zimmerman, 2010). Damming represents the most prevalent form of hydrological alteration. About 60 % of the world's rivers are fragmented by flow regulation through impoundment (Shao et al., 2020; Zeiringer et al., 2018). River regulation causes homogenization of river dynamics, alteration of baseflow, and greater flooding, in terms of magnitude, timing, frequency, and floodplain inundation (Dynesius and Nilsson, 1994; Mustonen, 2017; Poff et al., 2007; Rolls and Bond, 2017). In-channel, riparian, and floodplain communities are influenced by variations in temporal and spatial flow conditions, which disrupts thermal regimes and sediment transport (Poff and Ward, 1989). Over the past several decades, >70 % of riparian wetlands have been degraded and dam construction has contributed to 44 % of this reduction (Zheng et al., 2019). Hence, studying alteration in river flow regimes is the first step in determining the extent of the total influence.

Several commonly used methods are available for assessing change in flow regimes (Guo et al., 2021; Magilligan and Nislow, 2005; Olden and Poff, 2003; Poff et al., 1997). The most widely used method, which provides valuable information regarding the impact of human activities and climate change on rivers, is the “Indicators of Hydraulic Alteration” (IHA) developed by The Nature Conservancy (Richter et al., 1996; Yan et al., 2021; Yang et al., 2017). The method and software work on daily hydrologic data, such as streamflow, river stages, groundwater levels, or lake levels. The power of the IHA method is that it can be used to summarize long periods of daily hydrologic data into a much more manageable series of ecologically relevant hydrologic parameters (TNC, 2009). The method that was mostly developed for arid and semi-arid regions with irrigated agriculture is called the River Impact (RI) method. It provides a comprehensive and straightforward framework for assessing the impact of climate and land-use change on stream flows in regions with high seasonal irrigation demand (Fazel et al., 2017; Torabi Haghighi et al., 2014).

Generally, the impact of human activities (i.e., river regulation and land-use change) has a cumulative effect from upstream to downstream and influences the lower area of the basin (Akbari et al., 2020; Ashraf et al., 2016; Fazel et al., 2017; Torabi Haghighi et al., 2021; Xu et al., 2021). The most striking example is the Aral Sea crisis caused by the growth of non-repayable water consumption for irrigation in the headwater and mid basin of the Amu Darya and Syr Darya Rivers feeding the lake. The dam construction along the rivers has significantly changed the natural flow regime, reducing the inflow into many terminal lakes in Iran (Akbari et al., 2019; Torabi Haghighi et al., 2020; Yaraghi et al., 2019). The 170 dams build on the rivers feeding Lake Urmia turned 70 % of what was once the biggest hypersaline lake in the Middle East into natural salt pans (Hamzekhani et al., 2016; Nourani et al., 2019; Torabi Haghighi et al., 2018; Tourian et al., 2015). Following the same fate due to dam-induced changes, such as decreased water flow, Lake Bakhtegan, with its riparian wetlands and Hamun Lakes on the Iran-Afghanistan border, faces a similar environmental crisis (Akbari et al., 2022).

The most sensitive ecosystems in terms of response to fluctuations in hydrological components are estuarine wetlands, particularly those in arid regions where mangroves and seagrasses exist near the limit of their tolerance to extreme temperature, precipitation, and salinity (Etemadi et al., 2021; Schile et al., 2016). Estuarine wetlands are ecotones between land and sea where freshwater meets seawater, forming one of the most valuable ecosystems worldwide (Baugh et al., 1990; Costanza et al., 1997; D. Liu et al., 2021b; Yang et al., 2019). Due to the special geographic position, the health and expansion of these biodiversity hot spots rapidly respond to the fluctuations in environmental variables caused by climate change or increased human activities on the mainland and in the sea (Adame et al., 2021; Pouladi et al., 2017). The physical process linkages between coastal and estuarine systems mean that changes in the management actions in either system can produce changes in the other (Pontee and Cooper, 2005). Ranasinghe (2020) highlights the need for integrated climate change impact assessments at various spatio-temporal scales to produce reliable support for local-scale coastal management/adaptation decisions. Many studies confirmed a climate change-induced shift or position change in many estuaries rather than a reduction in their extent (Bamunawala et al., 2021; Smith et al., 2013). However, the relationship of estuarine wetland dynamics with sea-level rise and hydrological alterations caused by dam operations has not yet been clarified, so it is not obvious which one is a dominant driver of change (Adame et al., 2021; Baker et al., 2011; Chi et al., 2018; Kennish, 2002; Lotze et al., 2006; Lovelock et al., 2017; Pouladi et al., 2017). Therefore, the evolution of these dynamic transition zones is better assessed by considering the entirety of the Catchment-Estuary-Coastal (CEC) systems (Bamunawala et al., 2021, 2020). Though there is considerable existing work on river flow alteration and its influence on riverine habitats (da Silva et al., 2020; Sanches et al., 2006; Stewardson et al., 2017), the question of the impact of dam operation on downstream estuarine wetlands has yet to be addressed (Yang et al., 2019; Zheng et al., 2019).

Facing these pressing problems, the study's primary goal is to provide scientific information for the conservation and management of estuarine wetlands. This study focuses on how hydrologic changes in upstream river regulation can affect lowland systems. We utilized long-term hydrologic data for the Mond river basin in the south of Iran to assess the hydrological change and possible influences on land cover change in the downstream estuarine zone, the Mond Protected Area (MPA). Specifically, the study aims to: (1) identify flow regime characteristic changes after the construction of dams; (2) determine the role of the unregulated mid-basin (subbasin below the main dams) in diminishing the impact of river regulation in the lower part of the basin; and (3) evaluate the extent to which the Mond protected area can be influenced by upstream river regulation.

2. Materials and methods

2.1. Study area

The Mond river basin (47,654 km^2) is a sub-basin of the Persian Gulf and extends into two southern provinces (Fars and Bushehr) of Iran (Torabi Haghighi et al., 2020). The Mond river is the fifth longest river in Iran and is considered to be a unique and main source of surface water in the central part of the Persian Gulf basin (Fig. 1-a). Agricultural activities are a primary source of livelihood for the local population, and the groundwater and surface water resources are under increasing pressure from rapidly growing demands and farm areas. Supplementary Material provides an overview of groundwater depletion in several aquifers across the Mond basin (Fig. 1-c). The Mond river network consists of several tributaries; this study focused on Qare-aqaj, Simakaan, Shoor Jahrom, Shoor Firouzabad, and Baqan tributaries (Fig. 1-b).

The history of river regulation covers >1700 years, when the Band Bahman was constructed to divert Qare-aqaj River flow for irrigation purposes (Torabi Haghighi et al., 2020). This ancient hydraulic structure still works as a diversion dam on the Qare-aqaj River. Due to the basin's high water demand, Mond river regulation has been planned using six storage dams and several auxiliary hydraulic structures. Out of the 6 storage dams, the Salman Farsi Dam (1.4 km3) and Tangab (0.2 km^3) have been under operation since 2006, and the Hiqer Dam was commissioned in 2020 (Torabi Haghighi et al., 2020).

In the lower part of the basin, the Mond River, before emptying into the Persian Gulf, feeds the Mond protected area (MPA), covering >50,000 ha (Fig. 1-b) (Etemadi et al., 2021). The Department of Environment of Iran has registered this region as a national park since 2010. It is one of the main habitats for *Gazella subgutturosa* and the wintering of birds such as flamingos (Iran Environment and Wildlife Watch, 2010). The MPA consists of three major habitats: the coastal, riverine, and inland zones (Mehrabian et al., 2009), which are essential for migratory birds, wildlife, and aquatic organisms, especially fish (Pouladi et al., 2017). The coastal zone is mainly filled with seawater without vegetation, and only southeastern parts of this habitat zone are covered by vulnerable mangrove forests (Mehrabian et al., 2009). Mangrove forest in the MPA is expanding landward due to the sea-level rising in the Persian Gulf by 4 mm per year (Etemadi et al., 2021).

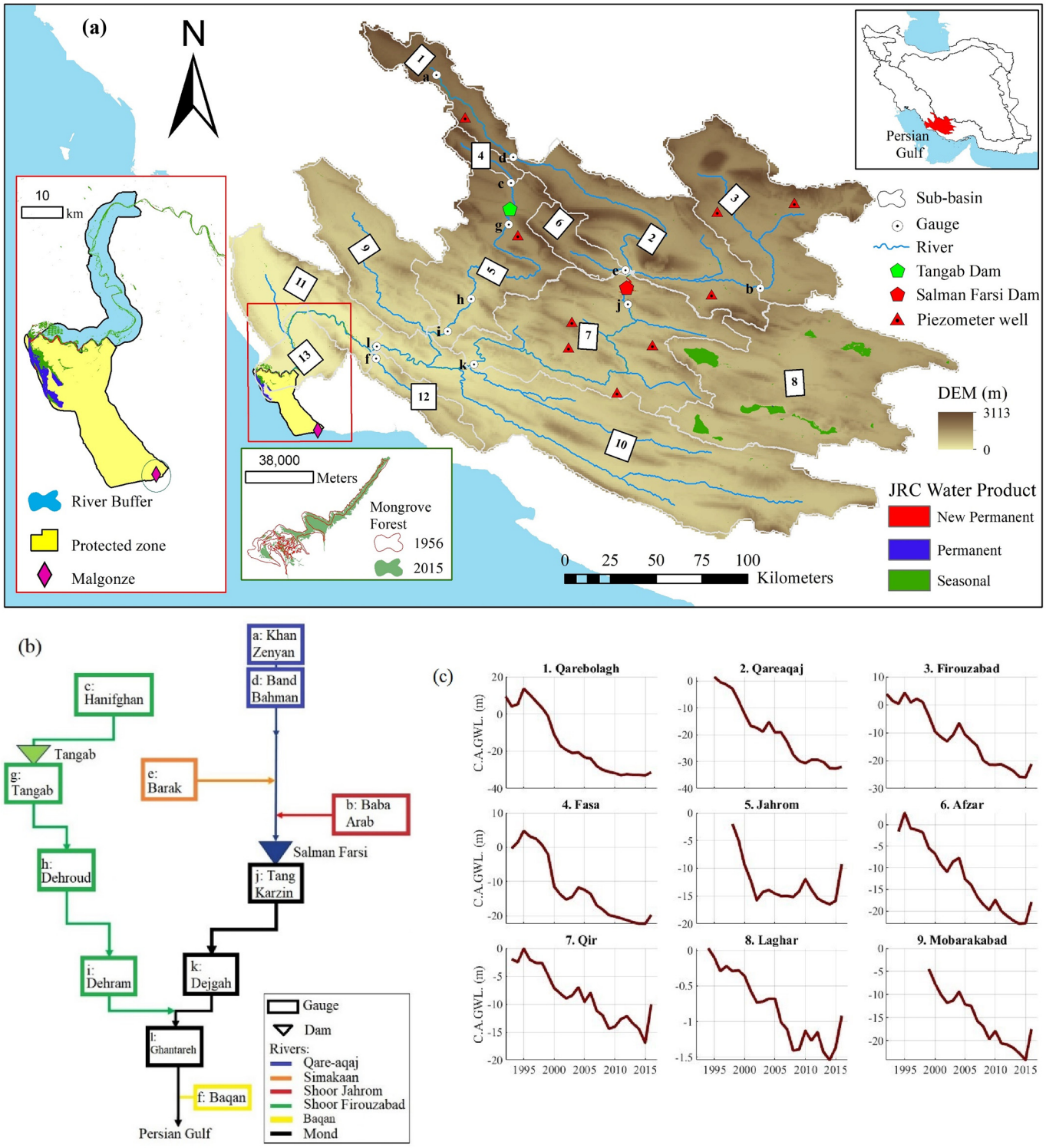

Fig. 1. a) Mond River sub-basins (id of each sub-basin from 1 to 13 in a box) with the location of gauges (ids of each gauge -from a to l next to it), b) river network of the basin, c) groundwater depletion in several aquifers across the Mond basin.

For example, in Malgonze (shown in Fig. 1-a), the mangrove forest has increased from 9.3 ha in 1956 to 11 ha in 2015 (Etemadi et al., 2021).

2.2. Data sets

As the primary purpose of this work is to assess the cause and effects of upstream-downstream river regulation, we select flow data from 12 gauges from 1987 to 2017 (Fig. 1-b and Table 1). These stations are divided into three spatial subcategories: upstream (Khan Zenyan, Baba Arab, Hanifghan, Band Bahman, Barak), midstream (Tangab, Dehroud, Dehram, Tang Karzin, Dejgah) and downstream (Baqan and Ghantareh). Tang Karzin and Tangab are immediately placed below the Salman Farsi (SF) and Tangab (Ta) dams. Although the Baqan is a headwater of a lowland sub-basin (Fig. 1-a), it is categorized as downstream because of its location. Based on the river network configuration, available gauges with proper flow data, and control points (e.g., dams and confluence points), the basin

Table 1
Names and coordinates of the gauges at the outlets of the sub-basins in the study area.

ID	Station	River	A km^2	Lon.	Lat.	Alt.	Comments
a	Khan Zenyan	Khatiri	196	52.15	29.67	1940	The headwater of the Qare-aqaj River
b	Baba Arab	Shoor J	4945	53.75	28.57	1100	The headwater of Shoor Jahrom
c	Hanifghan	Shoor F	422	52.55	29.12	1590	The headwater of Shoor Firouzabad
d	Band Bahman	Qare-aqaj	1586	52.58	29.22	1650	Headwater and near Kavar Dam
e	Barak	Simakaan	875	53.15	28.65	860	Headwater tributary
f	Baqan	Baqan	923	51.87	28.23	70	Last tributary of Mond before the PG
g	Tangab	Shoor F	1372	52.53	28.92	1310	Below Ta Dam
h	Dehroud	Shoor F	2489	52.57	28.62	870	Haiqer Dam place
i	Dehram	Shoor F	3844	52.35	28.48	415	Last station on Shoor Firouzabad
j	Tang Karzin	Mond	12610	53.12	28.48	740	Below SF Dam
k	Dejgah	Mond	18326	52.35	28.18	200	Downstream
l	Ghantareh	Mond	35353	51.87	28.25	80	Last station on the main river

F:Firouzabad, J:Jahrom, A:Area, Lon: Longitude, Lat: Latitude, Alt: Altitude, PG: Persian Gulf.

was divided into 13 sub-basins (sub-basins 1–13, Fig. 1-a). The flow data from 12 gauges (Fars regional water authority) were used for the flow regime analysis across the Mond basin (points a-l, Fig. 1, Table1). The daily data for 11 gauges was available from national datasets maintained by Fars regional water authority, while only monthly data was available for Khan Zenyan gauge (a), which was obtained from the Iranian water resources management company.

We retrieved potential evaporation and precipitation data in the Mond River basin sub-basins from the ECMWF ERA5 product. ERA5 is a re-analysis dataset that gives a detailed record of the global atmosphere, land surface, and ocean waves from 1950 onwards (Hersbach et al., 2020). The Terra and Aqua combined Moderate Resolution Imaging Spectroradiometer (MODIS) Land Cover Type (MCD12Q1) Version 6 was used to produce the land cover map, including sterile land, cropland, grassland, shrubland, urban, and water (Friedl and Sulla-Menashe, 2019).

Finally, the JRC dataset was used to produce the Spatio-temporal distribution of surface water from 1984 to 2019 across the basin (Pekel et al., 2016). To access all the above-mentioned data, we used the Google Earth Engine (GEE) JavaScript API online platform (Gorelick et al., 2017).

2.3. Methodology

This work will focus on each section of the CEC system, starting with river regime alteration in the entire catchment and progressing to its impact on estuary and coastal areas. The methodology includes several parts (Fig. 3). First, the spatio-temporal alteration in daily, monthly, and annual flow from upstream to downstream was analyzed using river impact (RI) and Indicator of hydrological alteration *(IHA)* methods. We used the standardized precipitation index (SPI) and the standardized potential evapotranspiration index (SPEI) to assess the possibility of climate change impact. We directly used available production in GEE to evaluate landcover change. Finally, we applied the Mann-Kendall test to evaluate the trend in inflow, precipitation, and potential evapotranspiration trends. Those applied methods are briefly explained as follows:

2.3.1. River impact method (RI)

Impacts on river flow can be seen as changes in river flow magnitude, timing, and intra-annual flow variability. Such changes were quantified by developing the impact factors MIF (magnitude impact factor), TIF (timing impact factor), and VIF (variation impact factor) (more details can be found in Torabi Haghighi et al., 2014) (see Fig. S3 in Supplementary Material (SM) for the concepts behind these factors). Dams can change one or more of these factors depending on their purposes. The combined RI factor considers all three major impacts:

$$RI = MIF \times (TIF + VIF) \tag{1}$$

The value of RI varies between 1 (the pre-impact period or the natural river flow regime) and 0 (the post-impact or completely changed river flow regime). The RI index range is defined by five different impact classes, where a value of 0.8–1.0 represents a 'low' impact (<20 % alteration in flow regime characteristics), 0.6–0.8 an 'incipient' impact, 0.4–0.6 a 'moderate' impact, 0.2–0.4 a 'severe' impact and 0.0–0.2 a 'drastic' impact (>80 % alteration in river flow regime). Based on the terms in Eq. 1, a graphical chart can be produced to visualize the river flow impact (Fig. S3).

The magnitude impact factor is calculated as:

$$\mathrm{MIF} = \mathrm{AF_{Post}}/\mathrm{AF_{Pre}} \tag{2}$$

where $\mathrm{AF_{Pre}}$ and $\mathrm{AF_{Post}}$ are mean annual flow in the pre-impact and post-impact periods, respectively for a specific gauging station.

Variation impact factor quantifies the variation in the hydrograph as:

$$IF = \frac{50 - 0.5 * I_{RR}}{100} \tag{3}$$

$$I_{RR} = \frac{|\, RRI_{Pre} - RRI_{Pos} \,|}{RRI_{Pre}} * 100 \tag{4}$$

where $\mathrm{RRI_{Pre}}$ and $\mathrm{RRI_{Pos}}$ are the River Regime Index (RRI) in the pre-impact and post-Impact periods, respectively, details of RRI calculation can be found in Torabi Haghighi and Kløve (2014).

Timing impact factor considers shifts in maximum, minimum, and 50 % of discharge cumulative density function (Torabi Haghighi et al., 2014)

$$IF = \frac{50 - 0.247 * TF}{100} \tag{5}$$

$$F = \frac{|\, DT_{Max} \,| + |\, DT_{Min} \,| + |\, DT_{Median} \,|}{3} \tag{6}$$

DTMax, DTMin, and DTMedian are the time shifts in monthly maximum discharge, monthly minimum discharge, and CDF50 timing value.

2.3.2. Indicator of hydrological alteration (IHA)

Daily water-discharge data was used to determine the influence of climate change and dam construction on the extent of hydrologic alteration in the Mond River Basin in terms of frequency, rate of change, timing, magnitude, and duration (Richter et al., 1998). The assessment was based on the IHA method, developed by Richter et al. (1996) using the default settings of the IHA7 software package (Version 7.1). Due to the skewed nature of the data non-parametric analysis was used and three RVA categories were established based on pre-impact flow percentiles: the low category, with values less than or equal to the 33rd percentile; the middle category, with values between the 34th and 67th percentiles; and the high category, with values greater than the 67th percentile (Richter et al., 1997). Thus, the degree of Hydrologic Alteration (HA) for all 33 IHA parameters is divided into three classes: 0–33 % (the light colour) represents little or no alteration; 34–67 % (the medium colour) represents moderate alteration; and 68–100 % (the dark colour) represents a high degree of alteration (Richter et al., 1998); these are summarized in a heat

map (Fig. 4). A negative Hydrologic Alteration value means that the frequency of values has decreased from pre-impact to post-impact with a minimum value of −1) (The Nature Conservancy, 2009).

As the studied hydrologic system has experienced an abrupt change due to dam construction, two-period analysis was used (The Nature Conservancy, 2009). It is common to use the date of reservoir completion as the impact year to divide the whole period into a pre-impact and post-impact period. Although the normal movement of water and sediment has interfered from the early stages of dam construction. Several years are needed to complete construction and fill the reservoir until it reaches the desired operating level. The date of dam closure, however, may not represent the time from which river regime alteration starts. Thus, it is logical to assume that the date when construction began represents this start time better. However, the magnitude of change is not significant at such an early stage. The Ta dam construction started in 2003 and ended in 2007 and the SF dam construction lasted longer as it started in 1995 and was completed in 2006. Therefore, to highlight the causes of river flow change and identify the breakpoint of streamflow in this study, we used the abrupt change-point detection technique based on the Pettitt test (Pettitt, 1979).

2.3.3. Drought analysis

For drought analysis, we utilized the Standardized Precipitation Index (SPI) and Standardized Precipitation-Evapotranspiration Index (SPEI) and used a Mann–Kendall trend test to quantify the significance of the drought characteristic trends at different time and space scales. Low data requirements and simplicity explain the wide use of the SPI for detecting and characterizing meteorological droughts (European Drought Observatory, 2020; Vicente-Serrano et al., 2010). The World Meteorological Organization has recommended that the SPI be used by all National Meteorological and Hydrological Services around the world (World Meteorological Organization, 2012). The SPI indicator was developed by McKee et al. (1993) and was described in detail by Edwards and McKee (1997). The SPI measures precipitation anomalies based on a comparison of observed total precipitation amounts for an accumulation period of interest with the long-term historical rainfall record for that period (European Commission, 2020). The SPEI is similar to SPI calculation but replaces precipitation with the difference between monthly precipitation and Potential-Evapotranspiration (PET) (C. Liu et al., 2021a). For any region, negative SPI values indicate meteorological droughts, while positive SPI values show severe excess rainfall (Mckee et al., 1993).

2.3.4. Land use/cover analysis

Land use is classified based on NDVI value. As the near-infrared (NIR) and red (RED) bands are strongly reflected and absorbed by plants, they are often used to represent the mangroves' health and photosynthetic activity (Kovacs et al., 2004). NDVI values range from −1 to 1, representing a reaction to photosynthetic activity, meaning that the higher the NDVI value, the greater the health and vegetation cover (Green et al., 1997). NDVI values close to 0 represent sparse vegetation or bare land, and values below zero are for wet soils and water (Etemadi et al., 2021). We used Landsat satellite images at a 30 m spatial resolution and 16-daily temporal resolution from 1990 to 2020 to calculate monthly NDVI at the end of the Mond River basin to see how vegetation cover changes.

3. Results

3.1. Abrupt change detection

As expected, the Pettitt test recognized different abrupt change years for regulated and unregulated river sections, and for all gauges, the detected year was significant, with $p < 0.01$ (a 99 % confidence level, Table 2). The results of the Pettitt test for the downstream stations of dams showed that the main corridor of the Mond River had been modified by the SF Dam since 2006 (almost the dam's commissioning year). There was a similar effect caused by the Ta dam on the Shoor Firouzabad River (a tributary of the Mond) since 2007. Whereas the change points for non-regulated rivers upstream and the last station downstream far from dams showed different years and were scattered between 1999 and 2008, showing the possible impact of climate and land-use change. The detected abrupt change year for one of the most upstream gauges (i.e., Baba Arab, change point: 03/01/1999) is close to the furthest downstream gauge (Ghantareh station, change point: 3/25/2000).

This study focused on the impact of dams on the downstream flow and the MPA. Therefore, to have a uniform and comparable flow regime alteration across the basin, the IHA and RI analyses were executed based on the year 2006, the abrupt change year below the SF dam, the largest reservoir in the Mond River basin (Table 2). Accordingly, all data was divided into a pre-impact (before 2006) and post-impact (after 2006) period.

3.2. Spatio-temporal change in the daily flow (IHA approach)

3.2.1. Changes to unregulated upstream

In this section, we focused on the Qare-aqaj river at Band Bahman, the Shoor Jahrom river at Baba Arab, the Simakaan river at Barak, and the Shoor Firouzabad River at Hanifghan (Fig. 1-b). Moderate to high HA levels of monthly flow alterations were observed across all studied gauging stations for the Mond River and its tributaries, as the river regime has changed from the pre-impact to post-impact period in all parts of the basin except the Shoor Jahrom tributary, which experienced the lowest level of alteration (Fig. 4, b). Result of the Pettitt test showed that the Baba Arab station experienced the change in 1999 (Table 2). This fact can be explained by the ephemeral nature of the Shoor Jahrom stream. It is difficult to evaluate the natural variability of an environment even on unregulated gauges because of the overexploitation of water resources (groundwater and surface water) throughout the basin. The mean annual daily flow has reduced significantly by 72 % in the post-impact period across four stations. The timing, magnitude, and duration of annual extreme water conditions have changed to moderate or high. In Hanifghan and Band Bahman, the timing of annual extreme water conditions has moved in opposite directions, the date of Julian annual maximum shifts by 20–21 days from January to February in Band Bahman and Baba Arab and by 10 days in January

Table 2
Detected abrupt change points across the Mond basin based on the Pettitt-test.

ID	Gauge	Impacting dam	Location	Change point	1-p	Pre-impact	Post-impact
b	Baba Arab	Non-Reg	USt	3/1/1999	1	1988–2005	2006–2017
c	Hanifghan	Non-Reg	USt	7/18/2006	1	1988–2005	2006–2017
d	Band Bahman	Non-Reg	USt	4/9/2008	1	1988–2005	2006–2017
e	Barak	Non-Reg	USt	5/9/2006	1	1988–2005	2006–2017
f	Baqan	Ba-D	DSt	6/23/2007	1	1977–2005	2006–2019
g	Tangab	Ta-D	MSt	5/23/2007	1	1988–2005	2006–2017
h	Dehroud	Ta-D	MSt	6/5/2007	1	1988–2005	2006–2017
i	Dehram	Ta-D	MSt	4/27/2007	1	1988–2005	2006–2017
j	Tang Karzin	SF-D	MSt	10/30/2006	1	1988–2005	2006–2017
k	Dejgah	SF-D	MSt	6/3/2006	1	1988–2005	2006–2017
l	Ghantareh	SF, Ta & Ba	DSt	3/25/2000	1	1970–2005	2006–2019

SF: Salman Farsi Dam, Ta: Tangab Dam, Ba: Baghan Dam, p: P_{value}, USt:Upstream, MSt: Midstream, and DSt: Downstream, Non-Reg: Non-Regulated.

for Hanifghan. Julian's date of annual minimum daily in the post-development period had been observed at 43, 55 and 22 days, earlier than the pre-development period, for Hanifghan, Band Bahman, and Barak, respectively, while this backward shift was only by one-day in the Baba Arab. In Hanifghan, Band Bahman, and Barak, low pulse count and duration increased, and high pulse count and duration decreased, which was the opposite with Baba Arab. There are high flow pulses, small and large floods during the highly wet 1994–1996 and 2004–2005 period, and an overall decrease in water flows after 2006 during the dry years. The November–April months have a high flow rate in the upstream stations, which corresponds to the "wet season" in this region as >95 % of precipitation falls then.

3.2.2. Impact of SF and Ta dams

To evaluate the impact of SF and Ta dams, we examined the flow regime alteration at Tang Karzin and Tangab gauges. Due to the operation of the SF dam in the Mond River, the magnitude of high flow has decreased. The minimum and maximum flow values were considerably reduced after the dam's construction. The magnitude of monthly streamflow parameters showed low to moderate HA levels; however, the July–October period increased river discharge. This is the opposite of the natural response of the river to the basin's climate pattern and confirms the impact of the dam's operation. One of the main purposes of the reservoir is to store water in the wet season and release it in the dry season for agriculture, as seen in the post-impact period. In January, such mean monthly values for the pre- and post-impact periods in Tang Karzin reduced from 41.98 m^3s^{-1} to 4.71 m^3s^{-1}, whereas in August, it increased from 2.44 m^3s^{-1} to 5.035 m^3s^{-1}.

The most remarkable change is observed below Ta dam at the Tangab station. The Ta dam has almost completely stopped water flowing into the valley, with around 90 % flow reduction. This is demonstrated by the increased number of zero-flow days from 19.21 in the pre-impact period to 307.9 in the post-impact period. Zero flow occurred from October 1993 to August 1994 and all months after 2008 with few exceptions during the winter months in 2009 and 2011. This increase in zero flow days is due to reservoir impounding and transferred water to the Firouzabad Plain for domestic and agricultural use. The post-impact period exhibited a high level of alteration in all IHA parameters, making the difference before and after dam construction clear. In the Tangab gauge, the mean annual flow decreased from 3.88 m^3s^{-1} to 0.16 m^3s^{-1}. However, the drastic effect tails off as it gets further from the Ta dam. Dehroud station (the nearest downstream station) has shown similar results, whereas the furthest station, Dehram, has demonstrated some differences with the increasing flow in the winter season.

3.2.3. Change in midstream stations (Dejgah, Dehram)

For the midstream, we analyzed the flow regime alteration on the Mond at Dejgah and Firouzabad at Dehram (Fig. 1). At these stations, the

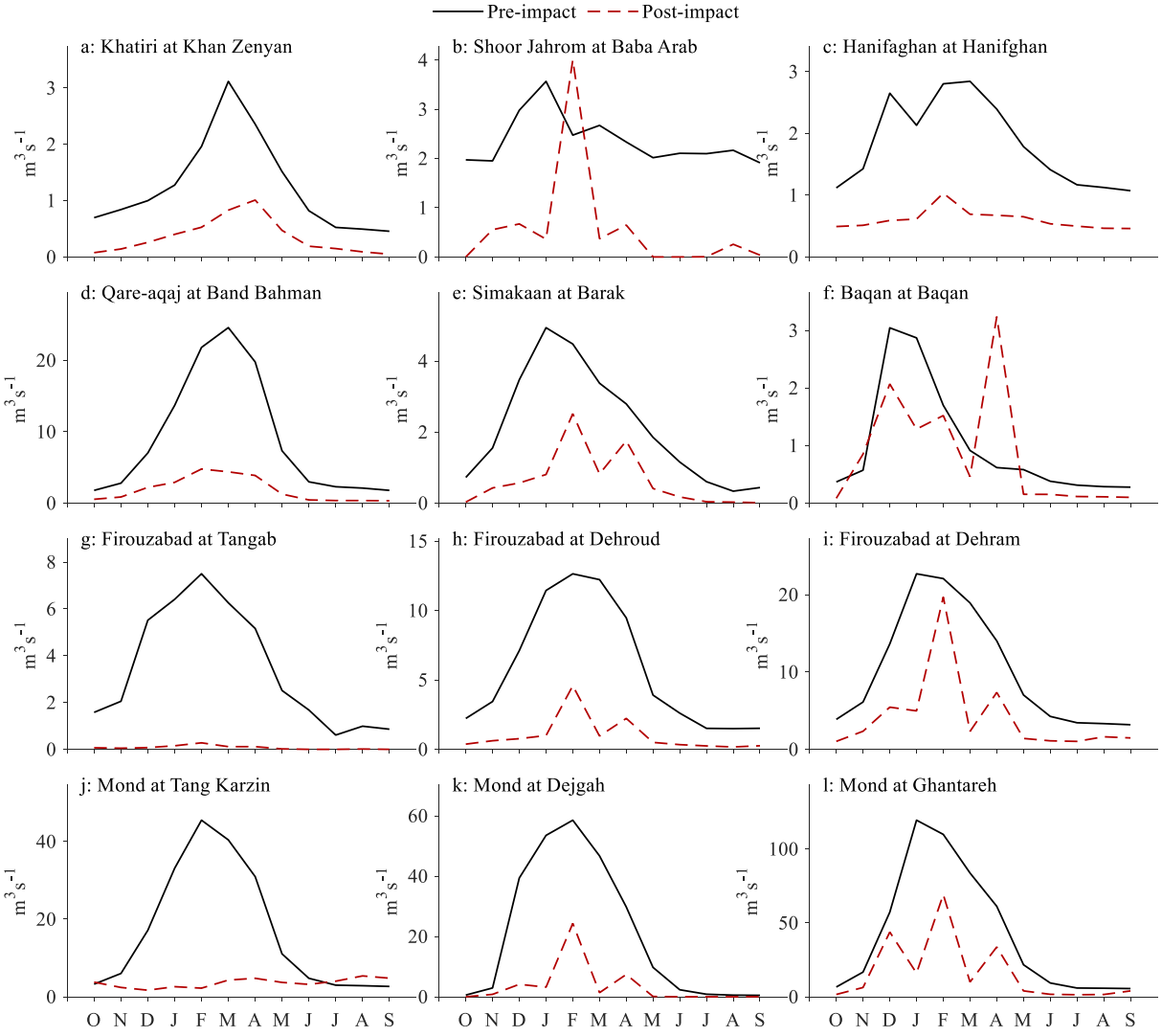

Fig. 2. Monthly flow in studied gauges for pre (1985–2005) and post-impact (2006–2015) periods.

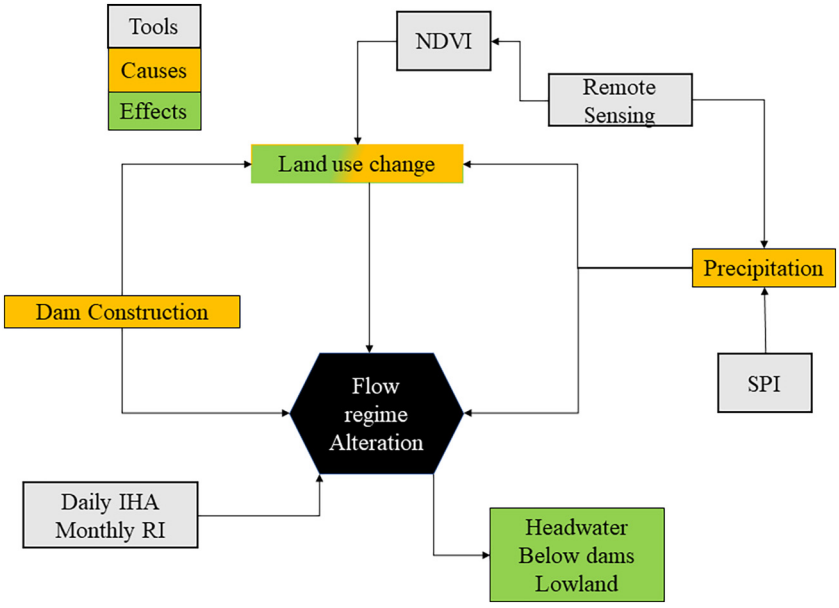

Fig. 3. Flow chart of Methodology.

differences between pre-and post-impact may be due to both the impact of climate change and reservoir operation. The post-impact hydrograph changed substantially, as most monthly flow indicators show a high degree of alteration from −0.66 to −1. Only in the winter months in Dejgah and Dehram is there a moderate level of HA magnitude. Compared with the pre-impact period, the mean value of the monthly flows in the post-impact period has changed considerably. For example, July's mean monthly flow in Dejgah in the pre-impact period was almost 0.9 $m^3s^{-1,}$ and after the dam construction, it fell to 0.00067 m^3s^{-1}. Similar results were observed at Dehram, from 1.13 m^3s^{-1} to 0.52 m^3s^{-1}. The dry season has extended as the month of peak discharge remains the same, whereas the date of minimum daily flow shifts from August to July for Dejgah station and from September to August station for Dehram.

For the extreme flow conditions, the average values of the minimum and maximum streamflow show a downward trend. During the post-impact period, the minimum flow rates for 7- and 30- days, and the baseflow index dropped to 0 in Dejgah due to the use of water for agriculture and overall water shortage in the region caused by the consecutive meteorological droughts. The maximum flows of 1-, 3-, 7-, 30-, and 90- days have also decreased. The number of days with zero flow has increased

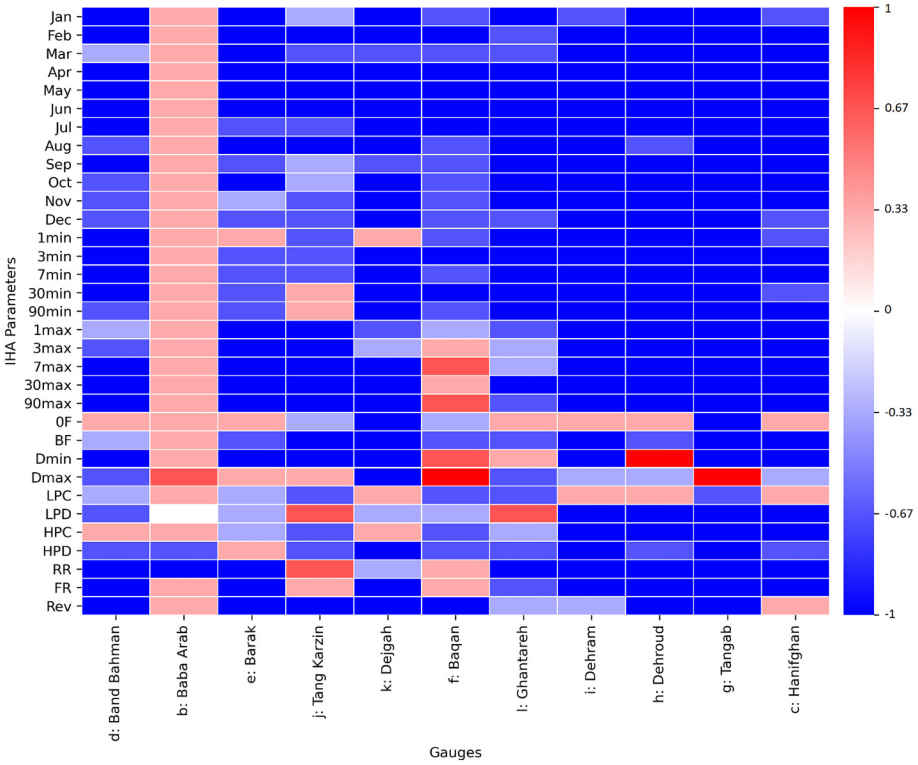

Fig. 4. Heat map of Indicators of hydrological alteration IHA for different Mond Sub-basins.

and covers half of the year in the Mond River, particularly after the 2000s. This may be due to anthropogenic activities and water use for irrigation, with the highest demand during the summer months. In contrast, there are no days with zero flow in Dehram on the Shoor Firouzabad River during the post-impact period. The maximum flow shows a moderate to high degree of change and the minimum flow shows a low-level alteration in Dejgah. In Dehram, all extreme flow conditions show high-level alteration. River flow regulation is the main driving force for the minimum flow, with climate change also possibly being responsible for reducing the maximum flow for 7-, 30-, and 90- days.

3.2.4. Change on downstream stations

Flow alteration levels at the two downstream gauges (Baqan and Ghantareh, Fig. 1-a) mostly varied between low and moderate levels. Even though the magnitude and duration of annual minima at these stations showed significant alteration which mostly reflected the climate and land-use change that impacted more low flow events than high flow, the magnitude, and duration of annual maxima were not affected in contrast to the highly altered high flow events at the Tang Karzin station (Fig. 4, l, f, j). High levels of HA of the monthly flow conditions were observed during the dry season, reflecting the water shortage during the vegetation season in Ghantareh (l) station, which is the opposite of the conditions in the midstream stations, where wet season flow was highly altered. This again shows how the midstream unregulated catchment greatly impacts the downstream area.

3.3. Spatio-temporal change in monthly flow (RI approach)

Of the 12 gauges, Tangab and Tang Karzin on the Shoor Firouzabad and Mond show the highest impact on flow regime, with a 0.02 and 0.08 RI index, respectively, indicating a 'drastic impact' (Fig. 5). This is due to the fact that these are located downstream of the Ta and SF Dams, respectively. Furthermore, two other gauges below these stations (Dejgah and Dehroud) also show a 'Drastic impact' on the flow regime, with a similar RI of 0.16 (Fig. 5). It shows that the additional flow in the mid-basin between Tang Karzin and Dejgah (about 5716 km^2, Table 1) on the Mond and between Tangab and Dehroud (about 1117 km^2, Table 1) on the Shoor Firouzabad River was not enough to dampen the impact of the two mentioned dams. In contrast, at the most downstream gauge (Ghantareh) of the Mond river basin, the RI was 0.35, and the impact level showed a moderated to sever impact (Fig. 5). This may be the result of the hydrological contribution of the large mid-basin area (about 20,254 km^2, Table 1) between Tangab, Tang Karzin, and Ghantareh gauges. This area includes three sub-basins: Kurdeh, Alamardasht, and Dashte-Pelang (Fig. 1-a, sub-basins 9 and 10).

The lowest impact on the flow regime was observed at Baqan station on the Baqan River (RI = 0.61, 'Incipient impact', Fig. 5). This river is the last lowland tributary (Altitude: 70 masl, Table 1) of the Mond river before joining the Persian Gulf. Furthermore, the two most upstream gauges on the headwater of the Qare-aqaj (Khan Zenyan at Khatiri, area: 195 km^2 and altitude: 1940 masl, Table 1) and Shoor Firouzabad (Hanifghan at Hanifghan, area: 422 km^2 and altitude: 1590 masl, Table 1) tributaries show a 'Sever impact' on the flow regime. Baba Arab station on the Shoor Jahrom had the highest impact (RI = 0.10, 'Drastic impact') among all headwaters. The flow regime of the Simakaan River (Fig. 2, e), which discharges as a tributary to the Qare-aqaj river just upstream of the SF dam, shows a 'Sever impact' (RI = 0.26, Fig. 5).

3.4. Spatio-temporal change in SPEI/SPI

Correlations of the annual SPI (Fig. 6) and SPEI (Fig. S1) from 1980 to 2020 for all basins in the studied area are very high (92–97 %). Therefore, we used annual SPI to investigate the climatic situation for each year. In Fig. 6 (as well as in Fig. S1), moderately to extremely wet years are shown as blue, mildly wet to moderately dry years as green, and moderately to extremely dry years as red. The high correlation between SPI and SPEI means that both indices resulted in a similar classification of years in terms of drought conditions. Therefore, for monthly drought estimation, we applied only SPI (Fig. S2). As shown in Fig. 6, from 1980 to 1995, SPI for the studied area has an increasing trend, but from 1995 to 2010 it decreases (except in the year 2004). 2010 is the driest year in the basin since 1980. After this (except for in 2016 and 2018), a continuous increase in SPI is observed in Fig. 6, similar to the period before 1995.

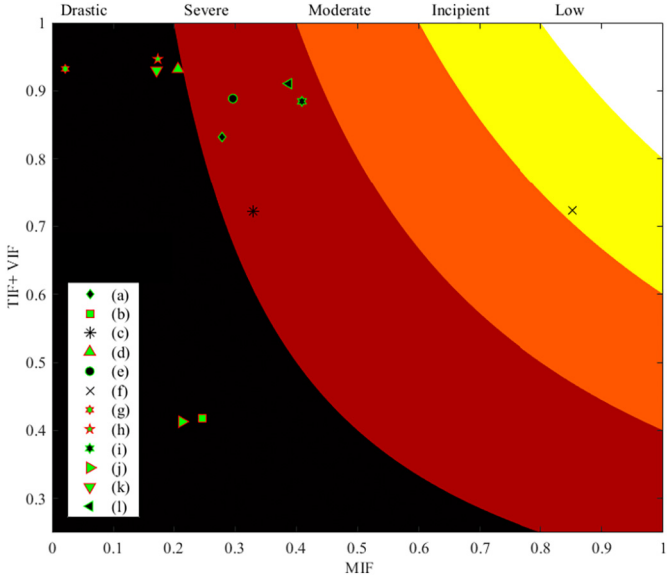

Fig. 5. Flow regime impact in different gauges across the Mond basin a: Khatiri at Khan Zanyan, b: Qare-aqaj at Band Bahman, c: Hanifaghan at Hanifghan, d: Shoor Jahrom at Baba Arab, e: Simakaan at Barak, f: Baqan at Baqan, g: Mond at Tang Karzin, h: Firouzabad at Tangab, i: Firouzabad at Dehram, j: Firouzabad at Dehroud, k: Mond at Dejgah and l: Mond at Ghantareh.

3.5. Land use/land cover change in the Mond Basin

Based on the land use map of 2019 from MODIS, the Mond River basin has five main land covers: barren, shrubland (hereafter called grazing), cropland, urban and water. Most of the studied area is covered by grazing (52.3 %) and barren (46.3 %) areas (Fig. 7). Also, 1 % of the basin consists of croplands, and <0.4 % is urban and water land cover. In the majority of sub-basins, a decrease in cropland was observed due to dry conditions (Fig. 8). From the upstream area of the Mond River basin to downstream, the share of grazing lands decreases, and barren areas dominate the sub-basins. For example, in the most upstream sub-basin, sub-basin 1, 96.7 % of the area is grazing and the rest is cropland. On the other hand, in the protected area (sub-basin 13), 87.8 % of the area is barren and 9 % is grazing lands (Fig. 7).

Over the basin, despite flow regulations and dam construction in recent years, the cropland area is decreasing (Fig. 8). SPI showed a decreasing trend from 2000 to 2010, but this trend became an increasing one after 2010. This variation in drought conditions for the studied area has affected barren land cover (Fig. S5). After 2010, barren land cover is decreasing in the majority of sub-basins. In 2018, barren land cover in the studied area increased suddenly, which can be attributed to low SPI (i.e., drought) in the basin. Increasing barren land cover from 2000 to 2010 and the decreasing trend after 2010 (except for in 2018), is the main pattern of land-use change in the Mond River basin. However, sub-basins 1, 8, and 10 do not follow this overall pattern, in these sub-basins grazing lands have been increasing continuously since 2000 regardless of drought conditions (Fig. S4). These three sub-basins are marginal and located upstream.

4. Discussion

4.1. Assessment of river regime change

Overall, both RI and IHA analysis for the Mond River clearly show that the change has occurred in the whole basin, from headwater to the lowland

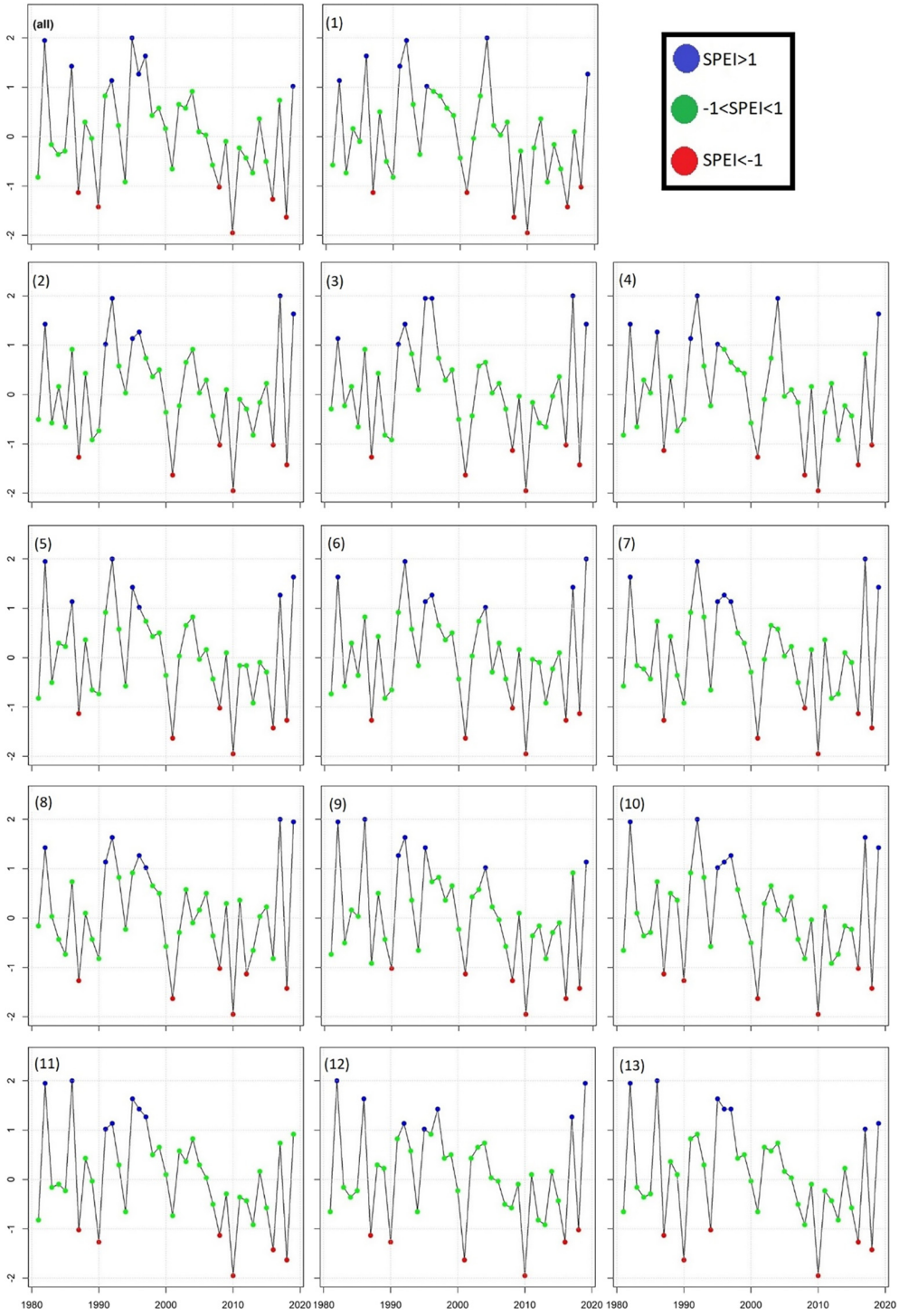

Fig. 6. Annual SPI in different sub-basins of Mond (based on annual and monthly precipitation from ERA5 in 1980–2020).

area. A spatio-temporal study on unregulated and regulated gauges reveals a decrease in river discharge during the post-impact period. This may be due to the overlapping of two drivers: i) the commissioning and impounding of dams (the SF and Ta) and ii) the meteorological drought from 2006 to 2010. For example, in Tang Karzin, below the SF dam, an increase in river discharge was recorded from July–October, which is the opposite of the natural and historical response of the basin to climate variability. In the pre-impact period, flow regime can be considered as the natural response of the basin to rainfall. During this period, most of the river discharge (about 95 % of mean annual flow) occurred during the rainy season (December–May). During the post-impact period, the maximum flow period is shifted to the crop's growing season (July–September) due to the dominating agricultural demand below the dam, and the release of stored water (during the flood season) in the SF dam (Torabi Haghighi et al., 2020). Even though the demand cannot be fulfilled with the current runoff and climate conditions (Karimi et al., 2016).

Furthermore, a negative trend in cropland area after 2000 indicates (Fig. 8) that the farming area has declined due to water shortage. This water shortage may be a consequence of the overexploitation of water resources (groundwater and surface water) and frequent hydrological droughts (Torabi Haghighi et al., 2020). After 1997, over-exploitation of groundwater became the leading source for irrigation of the developed,

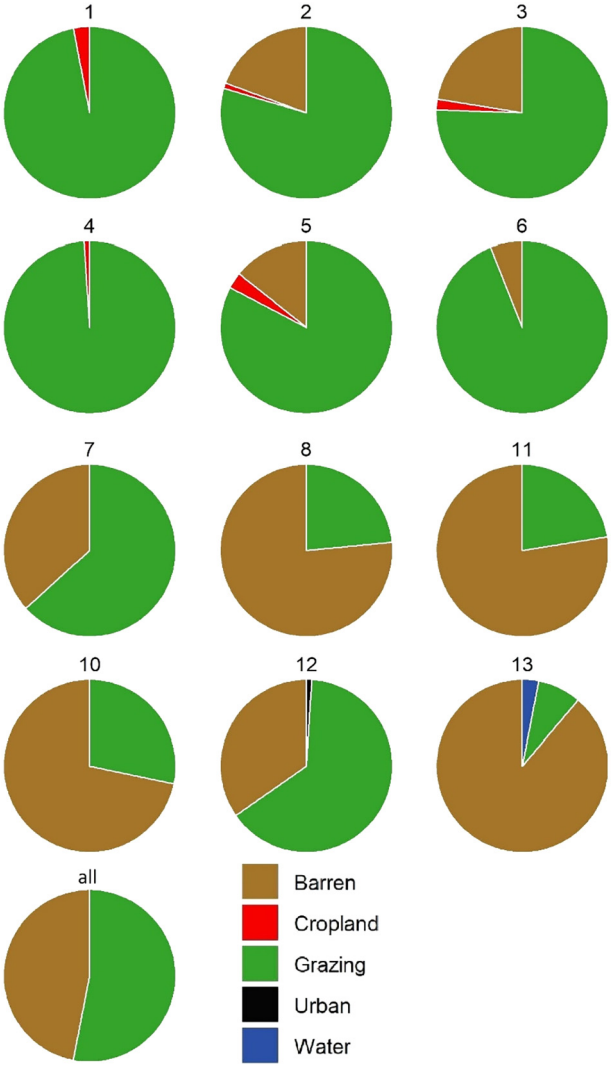

Fig. 7. Land cover in each sub-basin of the Mond River basin.

cultivated lands, leading to a significant depletion of aquifers Figs. S3) (Torabi Haghighi et al., 2020). The Shoor Jahrom and Shoor Firouzabad headwater tributaries of the Mond River are mainly fed by groundwater. The drastic and severe impact of the flow regime in Baba Arab and Hanifghan indicates the significant role of groundwater depletion (as the main driver of surface water availability) in these two sub-basins.

In contrast to the cropland, the grazing area has increased or changed (Fig. S4). This fluctuation pattern shows how the grazing area is a function of precipitation in the study area. In 2017 and 2019, the area of grazing was greater than in 2010 and 2018, which can be interpreted based on the amount of annual rainfall during these years (i.e., meteorological drought conditions).

The greatest flow regime alteration (the lowest RI value, RI: 0.02, drastic impact) was observed in the Shoor Firouzabad tributary of the Mond River below the Ta dam, and, due to this fragmentation, the river lost its natural connectivity. Despite this drastic impact at the Ta Dam's location, the impact of the Ta dam on the overall flow of the Mond River is minor and can be ignored. This issue can be confirmed by observing the impact on the next gauges on this river (Dehroud and Dehram, Fig. 1-h and i). The RI value in the Shoor Firouzabad river increased from 0.02 at Tangab to 0.16 and 0.36 at the Dehroud and Dehram gauges (Fig. 5). In these two stations in the midstream of the Mond basin, the level of alteration was like the unregulated upstream gauges of the river, i.e., Hanifghan station (Fig. 4-c). This recovery in the downstream flow regime is due to the contribution of unregulated mid-basin areas to the river flow. The mid basin area for the Dehroud and Dehram gauges covers 1117 (2489–1372) and 2472 (3844–1372) km^2, respectively (Table 1). Following the Tangab gauge on the Shoor Firouzabad, the flow regime at Tang Karzin shows the highest impact on the flow regime (RI = 0.08). The SF dam on the Mond River is much bigger than the Ta dam and has had the greatest influence on the magnitude and duration of annual extreme water conditions. Likewise, similar to river conditions below the Ta Dam, the RI value at the Dejgah gauge (the lower mid basin gauge) increased to 0.15 (from 0.08 at Tang Karzin) (Fig. 5), which may be a result of increasing the area of the basin from 12,610 to 19,362 km^2. In terms of the flow regime impact, the Mond river at Dejgah is still classified as having a 'Drastic impact'. However, the flow regime at the Ghantareh station (the last gauge before the Mond Protected area) was well recovered (RI = 0.35) by the contribution of the mid-basin area. The flow in this gauge is the aggregation of the Mond river flow, the Shoor Firouzabad and two big seasonal sub-basins named Kurdeh and Darolmizan (sub-basins 7, 5, 9, and 10, Fig. 1-a). At this station, the RI value (0.35) is even higher than the RI value in all Mond headwaters, i.e., Hanifghan (0.23), Baba Arab (0.10), Khan Zenyan (0.23) and Barak (0.26). The IHA analysis for the last station (Ghantareh) showed similar results, showing the reduction of the impact of the upstream dams and recovery potential of the large mid-basin.

Even though the extent of alteration diminishes moving from the dams to downstream stations and the impact of the upstream dam operation was partially neutralized due to the addition of the unregulated catchment, the Mond does not fully recover, and the impact on the riverine ecosystem is still considerable. In general, the SF dam on the Mond river has dramatically diminished the seasonal and interannual streamflow variability and has resulted in the homogenization of river dynamics. The minimum and maximum flow values, the rates of rising and fall, and the magnitude of high flow have all decreased. The trapping of sediments and nutrients further impacts the river's biogeochemical processes and MPA. On the other hand, because of the SF dam induced flow homogenization, the river buffer zone and riparian wetland are no longer subject to periodic flooding events, particularly in low return periods, supporting the development of stable vegetation on the older alluvial soils. Reducing the baseflow and controlling the flood with low return periods leads to the shrinking of the floodplain area in MPA; therefore, the inhabitants use the floodplain for nutrition and watering. Extreme flow, particularly from the unregulated mid-basin, results in sudden inundation and animals becoming trapped in the flooded zone. For example, during an extreme event in 2018, several deer (*Gazella subgutturosa*) were trapped in a muddy flooded zone and died (Abbasi and Etemadi, 2021).

4.2. Assessment of the Mond Protected zone

As shown in Figs. S6 and S7, the water coverage area in sub-basin 13 is increasing due to sea-level rise in the Persian Gulf. >48.47 km of MPA was inundated by a sea-level rise during the years 1987–2015 (Taghavi Moghadam et al., 2018). Although we observed a consistent decrease in the seasonal water bodies (due to a lack of rainfall from 1995 to 2001) in this region, the area of permanent and seasonal water has had an increasing trend after 2001; this may be due to the >1000 ha of shrimp pools in this region in 2000. On the other hand, we cannot see any increasing trend in water area in the western sub-basin, sub-basin 8 (shown in Fig. 1-a), which was included in the analysis as a control site due to the natural water bodies that are not linked to the Mond River and are not affected by the dams. The area of water bodies in this sub-basin is a function of climate. In extreme wet years, e.g., 2017, water bodies expand due to floods or shrink in years with arid conditions, e.g., 1987 and 1990 (Fig. S6).

The monthly box plots based on NDVI (1990–2020) show how SPI conditions can affect the average NDVI in each region of MPA (Fig. 9). In most months of the year, higher SPI is more probable to result in a higher average NDVI in each zone of the MPA (zones are shown in Fig. 1-a). It should be noted that overlap between different classes of SPI in categorizing NDVI value is higher in the wet season (November, December, and January) compared to other months. Furthermore, SPI classes could not classify the

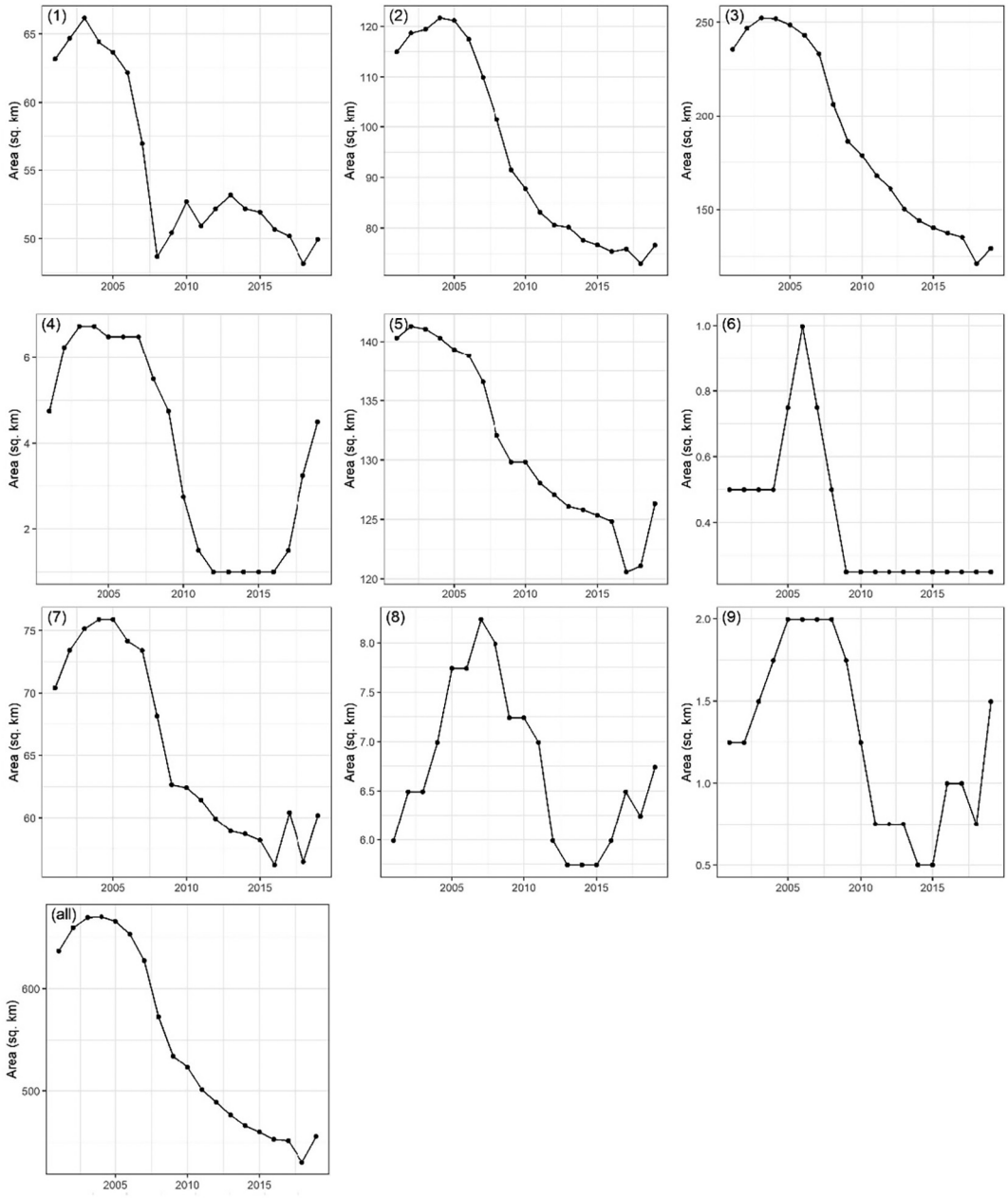

Fig. 8. Cropland change in different sub-basins of the Mond River basin.

average NDVI in protected area zone because, in this region, NDVI is affected greatly by Persian Gulf water, so the overlap of SPI classes is high and NDVI values are close to or less than zero, meaning the majority of the protected area is covered by negative NDVI value water. The Persian Gulf is connected to the Indian Ocean, and its level fluctuation is not considerably affected by SPI conditions in the small Mond basin. The average NDVI in other zones (river buffers west and east of the Mond River) is higher than zero and the river buffer has a higher NDVI than the west and east river zones. This is because of the concentration of farmlands in the river buffer zone. Comparing river buffer conditions before and after 2006, we conclude that after 2006, this region has a lower NDVI value average (i.e., less vegetation cover), especially when SPI is more than zero. Before 2006, blue boxplots in the river buffer zone are greatly above 0.1 but after 2006 they are <0.1. Similarly, after 2006, NDVI values in protected area zones shifted downward to more negative values because of sea-level rise, as discussed in the literature (Etemadi et al. 2020).

4.3. Limitations and uncertainties

Gaps in available data and the shortage of stream gauge record length may limit the sensitivity of RVA results. As the IHA manual considers 20 years as a reasonable baseline requirement, the validity of the IHA assessment should be carefully considered. In this study, the pre-impact period for the Shoor Firouzabad River was defined between 1988 and 2005 (17 years), such a short period can lead to skewed results due to climate variability and a few hydrologically extreme years. For the post-impact period, a data length (11 years) is sufficient (Zhou et al., 2021).

Retrieving precipitation and potential evaporation data for different sub-basins of the Mond River basin from the ERA5 reanalysis model was a source of uncertainty in this study. We used this data set because it is the last version of the reanalysis model of ECMWF, which has a high temporal and spatial resolution and good coverage from 1980 to 2020. Additionally, land use data, MCD12Q1 version 06, contain uncertainties. In areas of

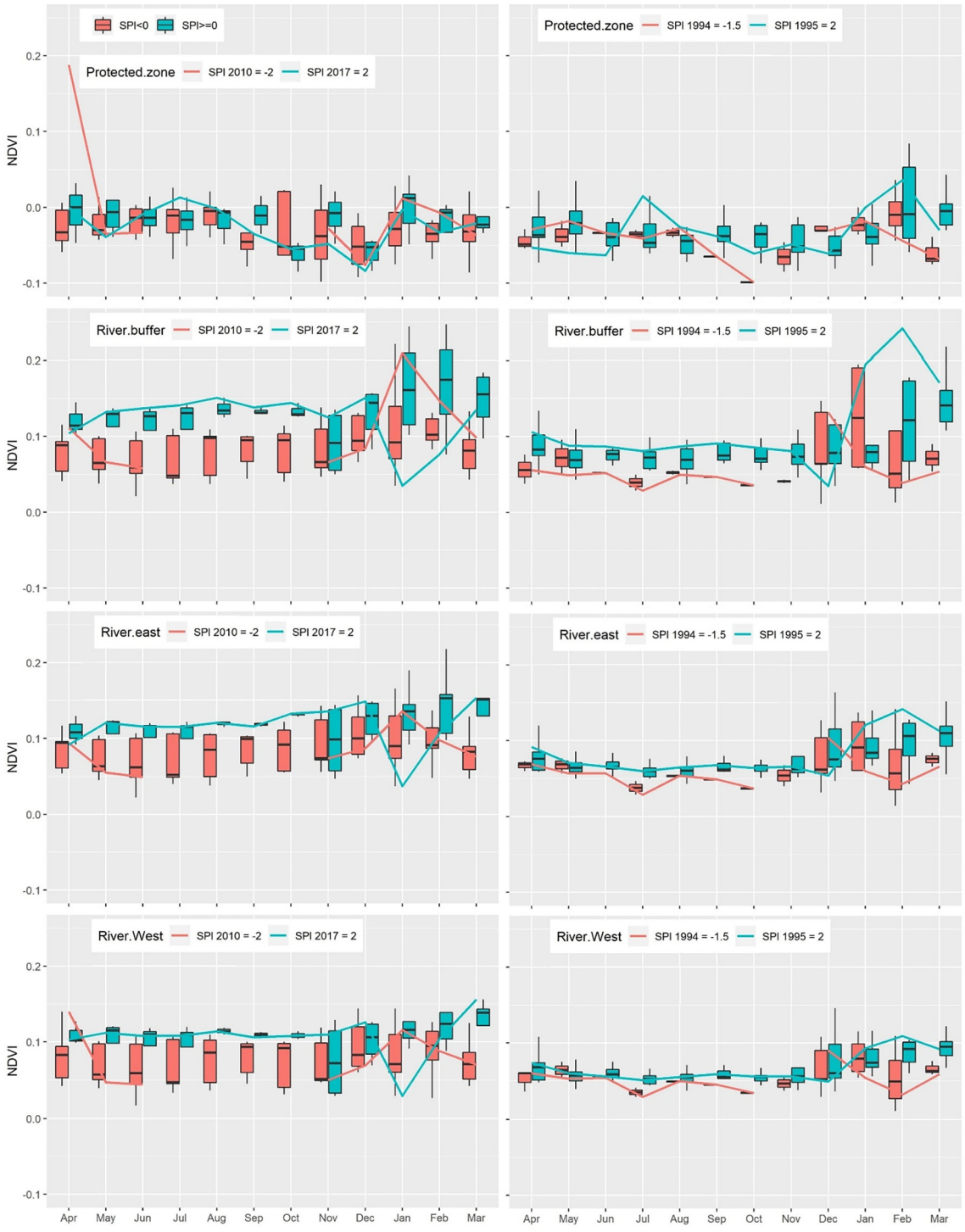

Fig. 9. Monthly change of NDVI in different regions of protected area based on monthly SPI two class conditions before and after 2006.

the tropics where cropland field sizes tend to be much smaller than a MODIS pixel, agriculture is sometimes underrepresented (i.e., labeled as natural vegetation), or some grassland areas are classified as savannas (sparse forest) (Sulla-Menashe and Friedl, 2018). We used this data set because it distinguishes between different land-use classes, providing valuable data for a change analysis from 2001 to 2019.

5. Conclusion

This study aims to broaden the coastal area assessment by considering the entirety of the Catchment-Estuary-Coastal (CEC) systems. Many studies discuss the negative impact of large dams on terminal lakes and riparian wetlands. Usually, the impact of human activities (i.e., river regulation and land-use change) can accumulate from upstream to downstream and influence the lower area of the basin. However, in the Mond CEC system, other drivers (e.i., rising sea level) were dominant drivers. Although the impact of the dams' operation on the river regime was drastic at gauges immediately after the dam commissions in 2006, it changed to a severe impact in the outlet of the basin. The prevailing barren and grazing land cover and low water consumption in the large mid-basin allowed the recovery of the flow regime below the dams. So, the impact of the flow regime at the last gauge (Ghantareh) is lower than the headwater and unregulated

parts of the river. Undoubtedly, with another layout of in-operation dams, regulating the bigger basin area and reducing the mid-basin area, the impact of river regulation was more in the last gauge on the Mond river. The rising sea level impacts the protected estuarine wetland more than the upstream river regime alteration and land-use change. The sea level rise in the coastal area increased water coverage and an inland vegetation shift. Furthermore, Remote sensing assessment shows that the NDVI is a function of SPI with higher vegetation cover during wet periods. Therefore, climate change and climate variability are the primary drivers influencing the MPA. The holistic approach and the basin-level study allowed us to assess the complexity of the drivers influencing the Mond Protected Area. Such comprehensive assessment gives a better understanding of drivers of change and can be used in communication with decision-makers to develop sustainable multi-scale coastal management plans.

CRediT authorship contribution statement

Aziza Baubekova: Conceptualization, Data curation, Methodology, Investigation, Formal analysis, Writing – original draft, Visualization, Project administration, Writing – review & editing. **Mahdi Akbari:** Investigation, Formal analysis, Data curation, Methodology, Writing – original draft, Visualization. **Hana Etemadi:** Data curation, Writing – review & editing, Validation. **Faisal Bin Ashraf:** Writing – review & editing, Validation. **Aliakbar Hekmatzadeh:** Investigation, Data curation. **Ali Torabi Haghighi:** Conceptualization, Methodology, Writing – original draft, Investigation, Formal analysis, Data curation, Supervision, Funding acquisition, Writing – review & editing.

Data availability

Data will be made available on request.

Declaration of competing interest

The authors declare that they have no known competing financial interests or personal relationships that could have appeared to influence the work reported in this paper.

Acknowledgements

This study was supported by Maa- ja vesitekniikan tuki ry (Reference Number: 41878).

Appendix A. Supplementary data

Supplementary data to this article can be found online at https://doi.org/10.1016/j.scitotenv.2022.160045.

References

Abbasi, I., Etemadi, H., 2021. Identifying areas affected by flood risk and providing operational solutions to reduce deer losses in the protected area. J. Environ. Sci. Technol. https://doi.org/10.22034/jest.2021.62927.5487.

Adame, M.F., Reef, R., Santini, N.S., Najera, E., Turschwell, M.P., Hayes, M.A., Masque, P., Lovelock, C.E., 2021. Mangroves in arid regions: ecology, threats, and opportunities. Estuar. Coast. Shelf Sci. 248. https://doi.org/10.1016/J.ECSS.2020.106796.

Akbari, M., Haghighi, A.T., Aghayi, M.M., Javadian, M., Tajrishy, M., Kløve, B., 2019. Assimilation of satellite-based data for hydrological mapping of precipitation and direct runoff coefficient for the Lake urmia basin in Iran. Water 11. https://doi.org/10.3390/W11081624.

Akbari, M., Baubekova, A., Roozbahani, A., Gafurov, A., Shiklomanov, A., Rasouli, K., Ivkina, N., Kløve, B., Haghighi, A.T., 2020. Vulnerability of the Caspian Sea shoreline to changes in hydrology and climate. Environ. Res. Lett. 15. https://doi.org/10.1088/1748-9326/ABAAD8.

Akbari, M., Mirchi, A., Roozbahani, A., Gafurov, A., Kløve, B., Haghighi, A.T., 2022. Desiccation of the transboundary Hamun Lakes between Iran and Afghanistan in response to hydro-climatic droughts and anthropogenic activities. J. Great Lakes Res. https://doi.org/10.1016/J.JGLR.2022.05.004.

Ashraf, F.Bin, Torabi Haghighi, A., Marttila, H., Kløve, B., 2016. Assessing impacts of climate change and river regulation on flow regimes in cold climate: a study of a pristine and a regulated river in the sub-arctic setting of Northern Europe. J. Hydrol. 542, 410–422. https://doi.org/10.1016/j.jhydrol.2016.09.016.

Baker, D.W., Bledsoe, B.P., Albano, C.M., Poff, N.L., 2011. Downstream effects of diversion dams on sediment and hydraulic conditions of Rocky Mountain streams. River Res. Appl. 27, 388–401. https://doi.org/10.1002/RRA.1376.

Bamunawala, J., Dastgheib, A., Ranasinghe, R., van der Spek, A., Maskey, S., Murray, A.B., Barnard, P.L., Duong, T.M., Sirisena, T.A.J.G., 2020. Probabilistic application of an integrated catchment-estuary-coastal system model to assess the evolution of inlet-interrupted coasts over the 21st century. Front. Mar. Sci. 7, 1104. https://doi.org/10.3389/fmars.2020.579203.

Bamunawala, J., Ranasinghe, R., Dastgheib, A., Nicholls, R.J., Murray, A.B., Barnard, P.L., Sirisena, T.A.J.G., Duong, T.M., Hulscher, S.J.M.H., van der Spek, A., 2021. Twenty-first-century projections of shoreline change along inlet-interrupted coastlines. Sci. Rep. 1 (11), 1–14. https://doi.org/10.1038/s41598-021-93221-9 2021 11.

Baugh, T.M., Day, J.W., Hall, C.A.S., Kemp, W.M., Yáñez-Arancibia, A., Yanez-Arancibia, A., 1990. Estuarine ecology. Estuaries 13, 112. https://doi.org/10.2307/1351438.

Chi, Y., Zheng, W., Shi, H., Sun, J., Fu, Z., 2018. Spatial heterogeneity of estuarine wetland ecosystem health influenced by complex natural and anthropogenic factors. Sci. Total Environ. 634, 1445–1462. https://doi.org/10.1016/j.scitotenv.2018.04.085.

Costanza, R., de Groot, R., Farberll, S., Grassot, M., Hannon, B., Limburg, K., Naeem, S., O, R.V., Paruelo, J., Raskin, R.G., Suttonllll, P., 1997. The value of the world's ecosystem services and natural capital. Nature 387, 253–260. https://doi.org/10.1038/387253a0.

Dynesius, M., Nilsson, C., 1994. Fragmentation and flow regulation of river Systems in the Northern Third of the world. Science 1979 (266), 753–762. https://doi.org/10.1126/science.266.5186.753.

Edwards, D.C., McKee, T.B., 1997. Characteristics of 20th-century drought in the United States at multiple time scales. Atmospheric Science Paper No. 634 Climatology Report No. 97-2 https://doi.org/10.17616/R31NJMSY.

Etemadi, H., Smoak, J.M., Abbasi, E., 2021. Spatiotemporal pattern of degradation in arid mangrove forests of the northern persian gulf. Oceanologia 63, 99–114. https://doi.org/10.1016/J.OCEANO.2020.10.003.

European Drought Observatory, 2020. Standardized Precipitation Index (SPI). Copernicus European Drought Observatory (EDO) , pp. 1–5. https://edo.jrc.ec.europa.eu/documents/factsheets/factsheet_spi.pdf. (Accessed 9 January 2022).

Fazel, N., Torabi Haghighi, A., Kløve, B., 2017. Analysis of land use and climate change impacts by comparing river flow records for headwaters and lowland reaches. Glob. Planet. Chang. 158, 47–56. https://doi.org/10.1016/j.gloplacha.2017.09.014.

Friedl, M., Sulla-Menashe, D., 2019]. MCD12Q1 MODIS/Terra + Aqua Land Cover Type Yearly L3 Global 500m SIN Grid V006. [dataset] https://doi.org/10.5067/MODIS/MCD12Q1.006.

Gorelick, N., Hancher, M., Dixon, M., Ilyushchenko, S., Thau, D., Moore, R., 2017. Google earth engine: planetary-scale geospatial analysis for everyone. Remote Sens. Environ. 202, 18–27. https://doi.org/10.1016/J.RSE.2017.06.031.

Green, E.P., Mumby, P.J., Edwards, A.J., Clark, C.D., Ellis, A.C., 1997. Estimating leaf area index of mangroves from satellite data. Aquat. Bot. 58, 11–19. https://doi.org/10.1016/S0304-3770(97)00013-2.

Guo, X., Xu, L., Su, L., Guo, Y., Deng, Y., 2021. A new method for assessing hydrologic alterations based on the discharge hydrograph. Hydrol. Sci. J. 66 (14), 2022–2032. https://doi.org/10.1080/02626667.2021.1971672.

Hamzekhani, F.G., Saghafian, B., Araghinejad, S., 2016. Environmental management in Urmia Lake: thresholds approach. Int. J. Water Resour. Dev. 32, 77–88. https://doi.org/10.1080/07900627.2015.1024829/SUPPL_FILE/CIJW_A_1024829_SM9012.PDF.

Hersbach, H., Bell, B., Berrisford, P., Hirahara, S., Horányi, A., Muñoz-Sabater, J., Nicolas, J., Peubey, C., Radu, R., Schepers, D., Simmons, A., Soci, C., Abdalla, S., Abellan, X., Balsamo, G., Bechtold, P., Biavati, G., Bidlot, J., Bonavita, M., De Chiara, G., Dahlgren, P., Dee, D., Diamantakis, M., Dragani, R., Flemming, J., Forbes, R., Fuentes, M., Geer, A., Haimberger, L., Healy, S., Hogan, R.J., Hólm, E., Janisková, M., Keeley, S., Laloyaux, P., Lopez, P., Lupu, C., Radnoti, G., de Rosnay, P., Rozum, I., Vamborg, F., Villaume, S., Thépaut, J.N., 2020. The ERA5 global reanalysis. Q. J. R. Meteorol. Soc. 146, 1999–2049. https://doi.org/10.1002/qj.3803.

Karimi, A., Torabi Haghighi, A., Klöve, B., Nikoo, M.R., Izady, A., Roozbahani, R., 2016. How multi-reservoir operation coordinating reduces impacts of The Kawar Dam's construction on Salman Farsi Dam' operation? International Water Conference 2016

Kennish, M.J., 2002. Environmental threats and environmental future of estuaries. Environ. Conserv. 29, 78–107. https://doi.org/10.1017/S0376892902000061.

Kovacs, J.M., Flores-Verdugo, F., Wang, J., Aspden, L.P., 2004. Estimating leaf area index of a degraded mangrove forest using high spatial resolution satellite data. Aquat. Bot. 80, 13–22. https://doi.org/10.1016/J.AQUABOT.2004.06.001.

Liu, C., Yang, C., Yang, Q., Wang, J., 2021. Spatiotemporal drought analysis by the standardized precipitation index (SPI) and standardized precipitation evapotranspiration index (SPEI) in Sichuan Province, China. Sci. Rep. 1 (11), 1–14. https://doi.org/10.1038/s41598-020-80527-3 2021 11.

Liu, D., Yu, H., Lu, K., Guan, Q., Wu, H., 2021. Freshwater releases into estuarine wetlands change the determinants of benthic invertebrate metacommunity structure. Front. Ecol. Evol. 9, 600. https://doi.org/10.3389/FEVO.2021.721628/BIBTEX.

Lotze, H.K., Lenihan, H.S., Bourque, B.J., Bradbury, R.H., Cooke, R.G., Kay, M.C., Kidwell, S.M., Kirby, M.X., Peterson, C.H., Jackson, J.B.C., 2006. Depletion degradation, and recovery potential of estuaries and coastal seas. Science 1979 (312), 1806–1809. https://doi.org/10.1126/SCIENCE.1128035.

Lovelock, C.E., Feller, I.C., Reef, R., Hickey, S., Ball, M.C., 2017. Mangrove dieback during fluctuating sea levels. Sci. Rep. 1 (7), 1–8. https://doi.org/10.1038/s41598-017-01927-6 2017 7.

Magilligan, F.J., Nislow, K.H., 2005. Changes in hydrologic regime by dams. Geomorphology 71, 61–78. https://doi.org/10.1016/j.geomorph.2004.08.017.

Mckee, T.B., Doesken, N.J., Kleist, J., 1993. The relationship of drought frequency and duration to time scales. Eighth Conference on Applied Climatology, pp. 17–22.

Mehrabian, A., Naqinezhad, A., Mahiny, A.S., Mostafavi, H., Liaghati, H., Kouchekzadeh, M., 2009. Vegetation mapping of the mond protected area of Bushehr province (South-West

Iran). J. Integr. Plant Biol. 51, 251–260. https://doi.org/10.1111/J.1744-7909.2008.00712.X.
Mustonen, T., 2017. Endemic time-spaces of Finland: from wilderness lands to 'vacant production spaces'. Fennia 195, 5–24. https://doi.org/10.11143/FENNIA.58971.
Nourani, V., Ghasemzade, M., Mehr, A.D., Sharghi, E., 2019. Investigating the effect of hydroclimatological variables on Urmia Lake water level using wavelet coherence measure. J. Water Clim. Chang. 10, 13–29. https://doi.org/10.2166/WCC.2018.261.
Olden, J.D., Poff, N.L., 2003. Redundancy and the choice of hydrologic indices for characterizing streamflow regimes. River Res. Appl. 19, 101–121. https://doi.org/10.1002/rra.700.
Pekel, J.F., Cottam, A., Gorelick, N., Belward, A.S., 2016. High-resolution mapping of global surface water and its long-term changes. Nature 540, 418–422. https://doi.org/10.1038/nature20584.
Pettitt, A.N., 1979. A non-parametric approach to the change-point problem. J. R. Stat. Soc.: Ser. C: Appl. Stat. 28, 126–135. https://doi.org/10.2307/2346729.
Poff, N., Ward, J., 1989. Implications of streamflow variability and predictability for lotic community structure: a regional analysis of streamflow patterns. Can. J. Fish. Aquat. Sci. 46, 1805–1818. https://doi.org/10.1139/f89-228.
Poff, N., Zimmerman, J., 2010. Ecological responses to altered flow regimes: a literature review to inform the science and Management of Environmental Flows. Freshw. Biol. 55, 194–205. https://doi.org/10.1111/j.1365-2427.2009.02272.x.
Poff, N.L.R., Allan, J.D., Bain, M.B., Karr, J.R., Prestegaard, K.L., Richter, B.D., Sparks, R.E., Stromberg, J.C., 1997. The natural flow regime: a paradigm for river conservation and restoration. Bioscience 47, 769–784. https://doi.org/10.2307/1313099.
Poff, N.L., Olden, J.D., Merritt, D.M., Pepin, D.M., 2007. Homogenization of regional river dynamics by dams and global biodiversity implications. Proc. Natl. Acad. Sci. 104.
Pontee, N.I., Cooper, N.J., 2005. The incorporation of estuaries within a strategic shoreline management framework. Proc. Inst. Civ. Eng. Marit. Eng. J. 158, 30–40.
Pouladi, M., Qadermarzi, A., Baharvand, F., Vazirizadeh, A., Hedayati, A.I., 2017. Effects of physicochemical factors on seasonal variations of phytoplankton in the Mond River Estuary of Bushehr Province, Persian Gulf, Iran. Biodiversitas J. Biol. Divers., 18 https://doi.org/10.13057/biodiv/d180130.
Ranasinghe, R., 2020. On the need for a new generation of coastal change models for the 21st century. Sci. Rep. 10, 2010. https://doi.org/10.1038/s41598-020-58376-x.
Richter, B.D., Baumgartner, J.V., Powell, J., Braun, D.P., 1996. A method for assessing hydrologic alteration within ecosystems. Conserv. Biol. 10, 1163–1174. https://doi.org/10.1046/j.1523-1739.1996.10041163.x.
Richter, B., Baumgartner, J., Wigington, R., Braun, D., 1997. How much water does a river need? Freshw. Biol. 37, 231–249. https://doi.org/10.1046/j.1365-2427.1997.00153.x.
Richter, B.D., Baumgartner, J.V., Braun, D.P., Powell, J., 1998. A spatial assessment of hydrologic alteration within a river network. Regul. Rivers Res. Manag. 14, 329–340. https://doi.org/10.1002/(SICI)1099-1646(199807/08)14:4<329::AID-RRR505>3.0.CO;2-E.
Rolls, R.J., Bond, N.R., 2017. Environmental and ecological effects of flow alteration in surface water ecosystems. Water for the Environment: From Policy and Science to Implementation and Management, Chapter: 4, pp. 65–83 https://doi.org/10.1016/B978-0-12-803907-6.00004-8.
Sanches, P.V., Nakatani, K., Bialetzki, A., Baumgartner, G., Gomes, L.C., Luiz, E.A., 2006. Flow regulation by dams affecting ichthyoplankton: the case of the Porto primavera dam, Paraná River, Brazil. River Res. Appl. 22, 555–565. https://doi.org/10.1002/RRA.922.
Schile, L.M., Kauffman, J.B., Fourqurean, J.W., Glavan, J., Patrick Megonigal, J., 2016. Limits on carbon sequestration in arid blue carbon ecosystems. Ecol. Appl. 27 (3). https://doi.org/10.1002/eap.1489.
Shao, X., Fang, Y., Cui, B., 2020. A model to evaluate spatiotemporal variations of hydrological connectivity on a basin-scale complex river network with intensive human activity. Sci. Total Environ. 723, 138051. https://doi.org/10.1016/J.SCITOTENV.2020.138051.
da Silva, G.C.X., Medeiros de Abreu, C.H., Ward, N.D., Belúcio, L.P., Brito, D.C., Cunha, H.F.A., da Cunha, A.C., 2020. Environmental impacts of dam reservoir filling in the East Amazon. Front. Water 2, 11. https://doi.org/10.3389/frwa.2020.00011.
Smith, T.J., Foster, A.M., Tiling-Range, G., Jones, J.W., 2013. Dynamics of mangrove-marsh ecotones in subtropical coastal wetlands: fire, sea-level rise, and water levels. Fire Ecol. 9, 66–77. https://doi.org/10.4996/FIREECOLOGY.0901066/FIGURES/9.
Stewardson, M.J., Acreman, M., Costelloe, J.F., Fletcher, T.D., Fowler, K.J.A., Horne, A.C., Liu, G., McClain, M.E., Peel, M.C., 2017. Understanding Hydrological Alteration. Water for the Environment: From Policy and Science to Implementation and Management, pp. 37–64 https://doi.org/10.1016/B978-0-12-803907-6.00003-6.
Sulla-Menashe, D., Friedl, M.A., 2018. User Guide to Collection 6 MODIS Land Cover (MCD12Q1 and MCD12C1) Product. https://doi.org/10.5067/MODIS/MCD12Q1.
The Nature Conservancy, 2009. Indicators of hydrologic alteration. Version 7.1 user's manual. https://www.conservationgateway.org/Documents/IHAV7.pdf. (Accessed 27 February 2022).
Torabi Haghighi, A., Marttila, H., Kløve, B., 2014. Development of a new index to assess river regime impacts after dam construction. Glob. Planet. Chang. 122, 186–196. https://doi.org/10.1016/j.gloplacha.2014.08.019.
Torabi Haghighi, A., Fazel, N., Hekmatzadeh, A.A., Klöve, B., 2018. Analysis of effective environmental flow release strategies for Lake urmia restoration. Water Resour. Manag. 32, 3595–3609. https://doi.org/10.1007/S11269-018-2008-3.
Torabi Haghighi, A., Sadegh, M., Behrooz-Koohenjani, S., Hekmatzadeh, A.A., Karimi, A., Kløve, B., 2020. The mirage water concept and an index-based approach to quantify causes of hydrological changes in semi-arid regions. Hydrol. Sci. J. 65, 311–324. https://doi.org/10.1080/02626667.2019.1691728.
Torabi Haghighi, A., Yaraghi, N., Sönmez, M.E., Darabi, H., Kum, G., Çelebi, A., Kløve, B., 2021. An index-based approach for assessment of upstream-downstream flow regime alteration. J. Hydrol. 600, 126697. https://doi.org/10.1016/J.JHYDROL.2021.126697.
Tourian, M.J., Elmi, O., Chen, Q., Devaraju, B., Roohi, S., Sneeuw, N., 2015. A spaceborne multisensor approach to monitor the desiccation of Lake urmia in Iran. Remote Sens. Environ. 156, 349–360. https://doi.org/10.1016/J.RSE.2014.10.006.
Vicente-Serrano, S.M., Beguería, S., López-Moreno, J.I., 2010. A multiscalar drought index sensitive to global warming: the standardized precipitation evapotranspiration index. J. Clim. 23, 1696–1718. https://doi.org/10.1175/2009JCLI2909.1.
Xu, F., Jia, Y., Niu, C., Sobkowiak, L., Zhao, L., 2021. Evaluating spatial differences in the contributions of climate variability and human activity to runoff change in the Haihe River basin. Hydrol. Sci. J. 66 (14), 2060–2073. https://doi.org/10.1080/02626667.2021.1974023.
Yan, M., Fang, G.-H., Dai, L.-H., Tan, Q.-F., Huang, X.-F., 2021. Optimizing reservoir operation considering downstream ecological demands of water quantity and fluctuation based on IHA parameters. J. Hydrol. 600, 126647. https://doi.org/10.1016/J.JHYDROL.2021.126647.
Yang, T., Cui, T., Xu, C.Y., Ciais, P., Shi, P., 2017. Development of a new IHA method for impact assessment of climate change on flow regime. Glob. Planet. Chang. 156, 68–79. https://doi.org/10.1016/J.GLOPLACHA.2017.07.006.
Yang, M., Lu, K., Batzer, D.P., Wu, H., 2019. Freshwater release into estuarine wetlands changes the structure of benthic invertebrate assemblages: a case study from the Yellow River Delta. Sci. Total Environ. 687, 752–758. https://doi.org/10.1016/J.SCITOTENV.2019.06.154.
Yaraghi, N., Ronkanen, A.Kaisa, Darabi, H., Kløve, B., Torabi Haghighi, A., 2019. Impact of managed aquifer recharge structure on river flow regimes in arid and semi-arid climates. Sci. Total Environ. 675, 429–438. https://doi.org/10.1016/j.scitotenv.2019.04.253.
Zeiringer, B., Seliger, C., Greimel, F., Schmutz, S., 2018. River hydrology, flow alteration, and environmental flow. In: Schmutz, S., Sendzimir, J. (Eds.), Riverine Ecosystem Management. Aquatic Ecology Seriesvol 8. Springer, Cham, pp. 67–89. https://doi.org/10.1007/978-3-319-73250-3_4.
Zheng, Y., Zhang, G., Wu, Y., Xu, Y.J., Dai, C., 2019. Dam effects on downstream riparian wetlands: the Nenjiang River, Northeast China. Water, 11 https://doi.org/10.3390/W11102038.
Zhou, X., Huang, X., Zhao, H., 2021. Uncertainty analysis for evaluating flow regime alteration of Jinsha River based on indicators of hydrologic alteration. Hydrol. Sci. J. 66 (12), 1808–1819. https://doi.org/10.1080/02626667.2021.1962882.